Contribution from the Fachbereich Chemie und Sonderforschungsbereich 127
der Philipps-Universität, D-3550 Marburg, FRG

Jahn–Teller Effect of Ti^{3+} in Octahedral Coordination: A Spectroscopic Study of $TiCl_6^{3-}$ Complexes

R. AMEIS, S. KREMER,† and D. REINEN*

Received July 24, 1984

Compounds $A_2A'TiCl_6$ (A, A' = alkali-metal ions) with cubic elpasolite structures have been investigated by means of ligand field, EPR, and Raman spectroscopy as well as susceptibility measurements and structural methods with respect to the Jahn–Teller instability of the octahedral $^2T_{2g}$ ground state. A strong dynamic coupling of the vibrational ϵ mode of the $TiCl_6^{3-}$ octahedra with this state is derived from the EPR data ($E_{JT} \approx 400$ cm^{-1}). Though the Ti^{3+} concentration is very large, no indication of a cooperative effect with a dynamic to static transition has been found down to 4.2 K. The phase transitions at 210 and 155 K for A, A' = Cs, K and Rb, Na, respectively, are caused by geometric packing forces and induce a tiny tetragonal distortion of the $TiCl_6^{3-}$ octahedra (D_{4h} compression), which superimposes on the otherwise dominating dynamic Jahn–Teller coupling. The splitting of the excited ^2E_g state in the ligand field spectra is also due to the ϵ mode. The vibronic interaction is much larger in this case ($E_{JT} \approx 1800$ cm^{-1}), because the ^2E_g state is σ antibonding and hence more strongly coupled to the ligand environment than the only π-antibonding $^2T_{2g}$ ground state.

Introduction

It is well-known that E_g ground states of transition-metal ions in octahedral coordination (d^9, d^4, low-spin d^7; vibronic $E \otimes \epsilon$ coupling)[1] undergo large splittings as the consequence of strong first-order Jahn–Teller effects, accompanied by (usually) static distortions of the ligand octahedra.[2-4] Not many investigations are concerned with the Jahn–Teller instability of T ground states in the same coordination geometry (d^1, d^2, d^6, d^7; low-spin d^4, d^5), however. Distortion effects are expected to be much less pronounced or even not present in these cases, because E_g states are σ antibonding, while T_{2g} states reflect only the π contributions to the metal–ligand bonds or are even nonbonding—depending on the nature of the ligands. The subject of this paper is the $^2T_{2g}$ ground state of Ti^{3+} in octahedral Cl^- coordination. We have chosen the ordered perovskite lattice $A_2A'TiCl_6$ (A = Cs, Rb; A' = Na, K) for our study, because it guarantees a host site of perfect octahedral geometry, if the structural tolerance factor is chosen properly. The preparation and further results of structural and ligand field spectroscopic measurements between 298 and 4.2 K are published elsewhere.[5,6] In this paper we report spectroscopic (EPR, IR/Raman) and magnetic measurements and also present the results of ligand field calculations with the inclusion of vibronic coupling, which are based on the available experimental data.

Experimental Section

Preparation. The elpasolite-type compounds $A_2A'TiCl_6$ were prepared by melting $TiCl_3$ and the alkali-metal chlorides in evacuated sealed quartz capsules. $TiCl_3$ was obtained by the reaction of Ti metal with $TiCl_4$. Because very small impurities will considerably affect the spectroscopic results (Figure 2), the preparation procedure—which is described in detail elsewhere[5]—had to pay attention to strict exclusion of even traces of air and humidity.

Spectroscopic and Magnetic Measurements. The diffuse-reflection spectra were recorded by a Zeiss PMQ II spectrometer (Infrasil) with a low-temperature attachment. We used freshly sintered MgO as a standard. The EPR spectra were taken with a Varian E 15 spectrometer (35 and 9 GHz) between 298 and 3.8 K with DPPH as the internal standard ($g = 2.003_7$). The Raman spectrum at 77 K (Figure 3) was kindly provided by the Inorganic Chemistry Department of Kiel University.

The magnetic measurements between 300 and 4.2 K were performed with a Foner magnetometer (calibration with $HgCo(NCS)_4$).

Results

a. $Rb_2NaTiCl_6$ (I) and Cs_2KTiCl_6 (II) are cubic elpasolites (space group $Fm3m$; $a = 10.26_5$ (I) and 10.76 Å (II)) and have geometric tolerance factors $t = 0.94$ and 0.92 (based on the ionic radii of Shannon and Prewitt),[7] respectively. They undergo second-order phase transitions to tetragonal unit cells at $T_c = 155$ (I) and 210 K (II) with c/a ratios of 1.01 (I) and $\simeq 1.02_5$ (II), which indicate only small deviations from the cubic structure.[5] Single-crystal X-ray data above and neutron diffraction powder data below T_c give evidence that the phase transitions are induced by geometric packing effects. The low-temperature structure results from rotations of the $TiCl_6^{3-}$ octahedra around a 4-fold axis. The temperature ellipsoids of Ti^{3+} and Cl^- are in accord with the rigid-ion model based on such motions.[5]

b. The ligand field spectra of compounds $A_2A'TiCl_6$ (Figure 1) show a more or less resolved double band ($^2T_{2g} \rightarrow {}^2E_g$ in O_h symmetry) at 11 900 ± 200 cm^{-1} with a splitting of 1400 ± 200 cm^{-1}.[6] They are indicative of strong vibronic coupling between the excited electronic E_g state and the ϵ_g normal vibration, because only this vibrational mode can lift the degeneracy of a doubly degenerate state and produce the observed band shape. A spectacular intensity decrease is observed when the temperature is decreased. At 4.2 K the remaining absorption is only very small and gives evidence for the presence of an inversion center of the $TiCl_6^{3-}$ polyhedra even at this low temperature.

c. In the EPR powder spectra (35 GHz) of I and II only a single line can be detected. At 4.2 K the signal of I is isotropic ($g = 1.58$) within the line width $\Delta H_{pp} = 500$ G (Figure 2). The signal of II is slightly anisotropic with $g_\perp > g_\parallel$ and the g components, as obtained from a line shape simulation procedure, are $g_\perp \simeq 1.58$ and $g_\parallel \simeq 1.50 - g_{av} \simeq 1.56$ (Figure 2). In a 3.8 K single-crystal study (9 GHz) we observed one (broad) signal with a small angular dependence; unfortunately the resolution was not sufficient to obtain the anisotropic components because of half-width reasons. Between 5 and 10 K the signals already become too broad for detection in both cases, obviously due to fast relaxation between closely neighbored vibronic levels (Figure 6). Rb_3TiCl_6 (III) has a distorted elpasolite structure already at 298 K ($t = 0.87$),[6] and the EPR signal at 4.2 K is distinctly split (Figure 2, III; $g_\perp = 1.60_7$ and $g_\parallel \simeq 1.44$–$g_{av} \simeq 1.55$). It is interesting to note that hydrolysis and/or oxidation leads to a new signal closer to g_0 (Figure 2, III'; $g_\perp = 1.85$). A strong axial component, induced by a Cl–O substitution in the neighborhood of the Ti^{3+} centers, is the presumable reason for this signal. If the compounds are not carefully handled during the measurements (strict exclusion of moisture and air), only the latter signal is observed (Figure 2, III').

EPR measurements (298 K) of the isomorphous Cr^{3+} compounds $Cs_2NaCrCl_6$ (high-pressure modification) and Rb_2Na-

† Present address: NBC Defence Research Institute, D-3042 Munster, GFR.

(1) M. C. M. O'Brien, *Proc. R. Soc. London, A*, **281**, 323 (1964).
(2) J. Gažo, I. B. Bersuker, J. Garaj, et al. *Coord. Chem. Rev.* **19**, 253 (1976).
(3) D. Reinen and C. Friebel, *Struct. Bonding (Berlin)*, **37**, 1 (1979).
(4) D. Reinen, *Comm. Inorg. Chem.*, **2**, 227 (1983).
(5) H. Wächter, W. Abriel, H. W. Mayer, and D. Reinen, *Z. Anorg. Allg. Chem.*, in press.
(6) P. Köhler, R. Ameis, and D. Reinen, to be submitted for publication.
(7) R. D. Shannon and C. T. Prewitt, *Acta Crystallogr., Sect. B: Struct. Crystallogr. Cryst. Chem.*, **B25**, 925 (1969).

0020-1669/85/1324-2751$01.50/0

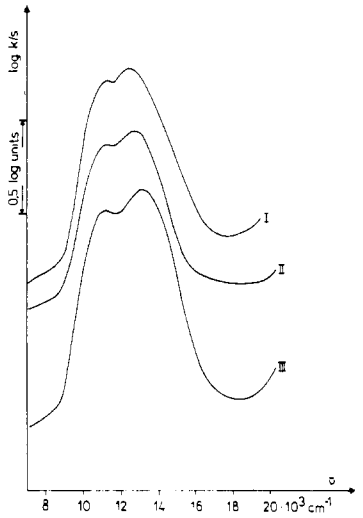

Figure 1. Ligand field reflection spectra (298 K) of $Rb_2NaTiCl_6$ (I), Cs_2KTiCl_6 (II), and Rb_3TiCl_6 (III).

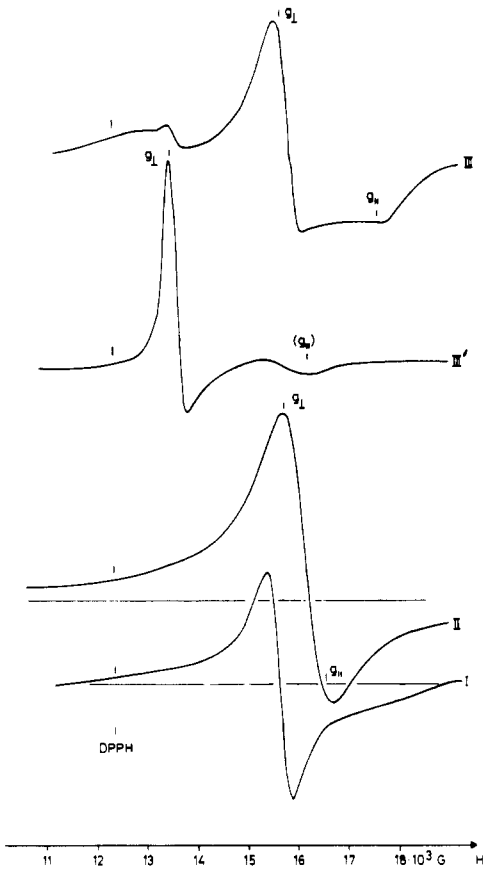

Figure 2. EPR powder spectra (34.8 GHz, 4.2 K) of $Rb_2NaTiCl_6$ (I), Cs_2KTiCl_6 (II), and Rb_3TiCl_6 (III, III') (III' = oxidized and/or hydrolized compound). DPPH ($g = 2.003_7$) is used as standard.

$CrCl_6$ yielded a narrow isotropic signal with $g = 1.98_4$.[6] From this value a covalency factor k' (cf. Discussion) of 0.57 is calculated, if eq 1 and the experimental values $\Delta = 13\,000$ cm^{-1} and $\lambda_0 = 90$ cm^{-1} (LS coupling constant of the free Cr^{3+} ion) are used.

$$g = g_0 - 8k'^2\lambda_0/\Delta \qquad (1)$$

From the three Kramers' doublets, which constitute the $^2T_{2g}$ ground state of octahedral Ti^{3+} (Figure 5), only the one that is designated with ${}_a\Gamma_7$ can lead to $g_\parallel$ and $g_\perp$ values near the spin-only value.[8] Because on the one hand the coupling to the ϵ_g mode is

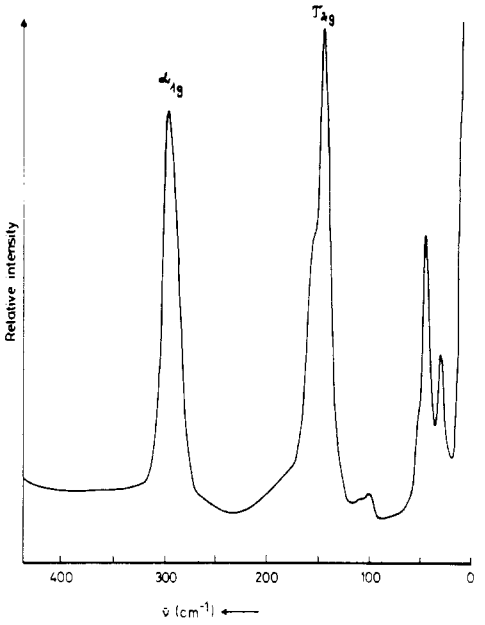

Figure 3. Raman spectrum (77 K) of Cs_2KTiCl_6 (assignment in O_h symmetry).

established by ligand field spectroscopy and because on the other hand the sign of the splitting parameter $3\delta_2$ determines which of the two Γ_7 ($^2T_{2g}$) doublets is lowest, only a tetragonal compression of the $TiCl_6^{3-}$ octahedra is in accord with the EPR experiment.

d. The far-IR spectra (298 K) of Cs_2KTiCl_6 ($Rb_2NaTiCl_6$) show clearly two broad, strongly asymmetric bands at 308 (312) and 125 (142) cm^{-1}, which have to be assigned to the two octahedral τ_{1u} modes. The corresponding bands of Cs_2KCrCl_6 are found at 329 and 135 cm^{-1}. The narrow band at 57 (72) cm^{-1} for Cs_2KTiCl_6 ($Rb_2NaTiCl_6$) cannot be assigned to the ϵ_u component of the inactive τ_{2u} vibration, which becomes allowed in D_{4h} symmetry; it also occurs (at 63 cm^{-1}) in the spectrum of Cs_2KCrCl_6, though the O_h symmetry of the $CrCl_6^{3-}$ octahedra down to 4.2 K is established by neutron diffraction.[5] For $(pyH)_3TiCl_6$ with a noncubic structure, band splittings are reported:[9] 300, 287 cm^{-1} and 184, 170 cm^{-1} (α_{2u}, ϵ_u from τ_{1u}). The band at 118 cm^{-1} is assumed to correspond to the ϵ_u (τ_{2u}) mode.

The Raman spectra (77 K) give clear evidence for band splittings of the τ_{2g} vibration (Figure 3), which is obviously due to the static D_{4h} distortion below the phase transition, mentioned before. For Cs_2KTiCl_6 the α_{1g} mode is observed at 304 cm^{-1}, and the split bands of the τ_{2g} mode are observed at 162 (ϵ_g component) and 151 cm^{-1} (β_{2g} component). The assignment of the split bands was based on the general observation that the nondegenerate components usually have the larger intensity. It leads—in accord with the previous results—to the conclusion that the $TiCl_6^{3-}$ octahedra are compressed. The ϵ_g vibration, which is expected to appear at somewhat lower energies than α_{1g} but distinctly above the τ_{2g} normal mode, is not seen. Possibly the weak band around 110 cm^{-1} is due to this mode, shifted to lower frequencies by vibronic coupling effects (see Discussion). In the Raman specrum of $Rb_2NaTiCl_6$ the bands are found at slightly higher energies, similar to those in the IR spectra. The α_{1g} band occurs at 314 cm^{-1}, while the split peak of the τ_{2g} band with the higher intensity is observed at 155 cm^{-1}. Though a distinct asymmetry with a shoulder on the higher energy side is evident, the ϵ_u component is not clearly resolved. Obviously the splitting of the τ_{2g} band is smaller than that for Cs_2KTiCl_6. This observation matches with the EPR result.

e. The susceptibility measurements yielded strongly temperature-dependent μ_{eff} values, as is demonstrated for Cs_2KTiCl_6 in Figure 4. The data for $Rb_2NaTiCl_6$ are very similar. The low-

(8) A. Abragam and B. Bleaney "Electron Paramagnetic Resonance of Transition Ions", Clarendon Press, 1970, p 417 ff.

(9) H. P. Fritz, W. P. Griffith, and G. Stefaniak, *Z. Naturforsch., B: Anorg. Chem., Org. Chem., Biochem., Biophys., Biol.*, **25B**, 2087 (1970).

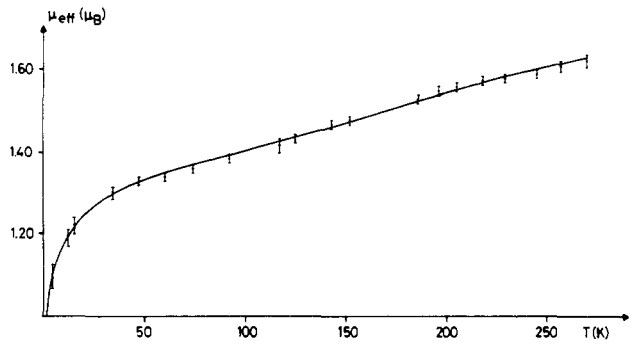

Figure 4. μ_{eff} vs. T curve for Cs_2KTiCl_6 (average over several measurements; only part of the experimental points included).

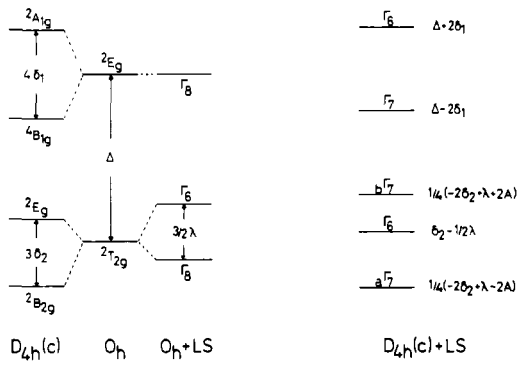

Figure 5. Energy level diagram of Ti^{3+} (d^1) in a static octahedral ligand field in the presence of LS coupling and a D_{4h} distortion component (compression) but without vibronic coupling (energies without $^2T_{2g}$–^2E_g interaction; $A = (9\delta_2 + 3\delta_2\lambda + {}^9/_4\lambda^2)^{1/2}$).

temperature μ_{eff} (1.10 ± 0.05 μ_B at 4.2 K) is smaller than the expected value $g(S(S+1))^{1/2} \simeq 1.33\ \mu_B$ (with $g = 1.56$) and is presumably caused by weak antiferromagnetic interactions between the Ti^{3+} ions in the elpasolite unit cell ($J \simeq 3 \pm 0.5$ cm^{-1}). This assumption is supported by magnetic data obtained for the isostructural $Rb_2NaCrCl_6$, where μ_{eff} is also reduced with respect to the expected value.

Discussion

a. The static ligand field calculation with a complete d^1 basis leads–with use of experimental values $\Delta = 11\,900$ cm^{-1}, $4\delta_1 = 1400$ cm^{-1}, $g_\parallel = 1.50$, and $g_\perp = 1.58$—to the parameters $3\delta_2 = 75$ cm^{-1} (Figure 5) and $k = 0.3$. The g values for the $_a\Gamma_7$ ground state are

$$g_\parallel = g_0 \cos 2\omega - k(1 - \cos 2\omega)$$
$$g_\perp = |{}^1/_2 g_0(1 + \cos 2\omega) - 2^{1/2}k \sin 2\omega| \qquad (2)$$

with $\cos 2\omega = (3\delta_2 + \lambda/2)/A$, $\sin 2\omega = 2^{1/2}\lambda/A$, $\lambda = k\lambda_0$, and A as defined in Figure 5. Second-order contributions Δg, which result from the $_{a,b}\Gamma_7(^2T_{2g}) - \Gamma_7(^2E_g)$ interactions (Figure 5), are negligible in the case of small k values ($\simeq$0.02; cf. Results, section c) and are not shown in eq 2. The parameter k is defined as usual[10] and describes the reduction of the LS coupling parameter $\lambda_0 = 190$ cm^{-1} and the angular moment L, due to covalency in the $^2T_{2g}$ ground-state multiplet. The calculated value of k is by far too low, however, to be explained by covalency alone, and is also far too low compared to k' of Cr^{3+} in the same environment ($k' \approx 0.6$; Results, section c).[11] Though the large line width of the EPR signals implies an error of ±0.05 for the g values at the utmost, this uncertainty would change k by only ±0.1 and still leave a covalency parameter that is too low.

So far we have not considered vibronic interactions. Though the orbital degeneracy of the T_{2g} ground state can equally be removed by ϵ_g and τ_{2g} vibrations, we consider only the coupling with the ϵ_g mode. The considerable splitting of the excited electronic E_g state gives evidence that the $T \otimes \epsilon$ interaction[12] is indeed of dominating influence. The inclusion of this dynamic coupling to first order in perturbation theory (adiabatic approximation) modifies k in eq 2, which is now the product of a vibronic (k_v) and covalency (k_c) contribution. The vibronic reduction is, according to Ham[12]

$$k_v(T_2) = e^{-3E_{JT}/2\hbar\omega} \qquad (3)$$

where $\hbar\omega$ is the energy of the ϵ_g vibration and E_{JT} the vibronic Jahn–Teller coupling energy within the T_{2g} state. With a covalency factor k_c of 0.6 (cf. Results, section c),[11] we calculate $k_v \simeq 0.5$ and hence $E_{JT} \simeq 0.45\ \hbar\omega$. With the arbitrary choice $\hbar\omega \simeq 250$ cm^{-1} (see Results, section d; usually the ϵ_g vibration is located between α_{1g} and τ_{2g}), one estimates $3E_{JT} \simeq 350$ cm^{-1}.[13]

We many hence conclude from these semiquantitative considerations that the structural and spectroscopic results indicate the following:

(A) A small static tetragonal compression of the $TiCl_6^{3-}$ octahedra due to geometric packing forces is present below the phase transition ($3\delta_2 \simeq 75$ cm^{-1}).

(B) Additionally, a dynamic $T \otimes \epsilon$ Jahn–Teller coupling is present, which lowers the energy of the ground state further by $2E_{JT} \simeq 250$ cm^{-1}.

For $Rb_2NaTiCl_6$ we obtain similar results, but with an even smaller $3\delta_2$ energy.

b. The calculation in section a of the Discussion was now refined by including second-order corrections due to the continuum of excited vibronic states (nonadiabatic approximation). The vibronic $T \otimes \epsilon$ coupling case has been treated by Ham.[12] We have taken account, in addition, of LS coupling in the $^2T_{2g}$, ^2E_g manifold, a static D_{4h} component, and the vibronic interactions of the ϵ-phonon states with the excited ^2E_g state. The influence of the last-mentioned interaction on the ground-state wave functions proved to be neglible in this case, however. By a proper choice of the vibronic functions in the basis set, the calculation allowed also for the fact that the three perturbations (λ, δ_2, E_{JT}) are of comparable magnitude. A detailed outline of the nonadiabatic ligand field model with vibronic coupling for octahedral Jahn–Teller ions in the presence of small tetragonal and trigonal ligand field com-

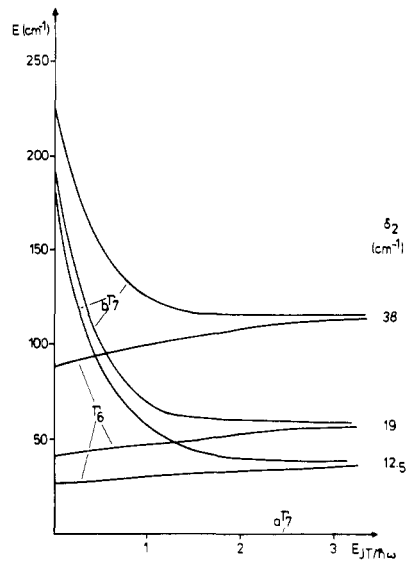

Figure 6. Energies of the three lowest vibronic levels vs. $E_{JT}/\hbar\omega$ for different δ_2 values (cm^{-1})—nonadiabatic ligand field model with $(T + E) \otimes \epsilon$ vibronic coupling to the ϵ-phonon continuum ($N \leq 17$) ($\Delta = 11\,900$ cm^{-1}; $k_c = 0.6$).

(10) K. W. H. Stevens, *Proc. R. Soc. London, A*, **A219**, 542 (1953).
(11) k' is partly due to covalency in the excited σ-antibonding ^2E_g state and should hence be smaller than k. For the sake of reducing the number of parameters in our calculations we have assumed $k' = k$.
(12) F. S. Ham, *Phys. Rev.*, **138**, A1727 (1965).
(13) $3E_{JT}$ is the splitting of the $^2T_{2g}$ ground state, if the Jahn–Teller effect is static, and describes the linear electron–phonon $T \otimes \epsilon$ coupling in the dynamic case.

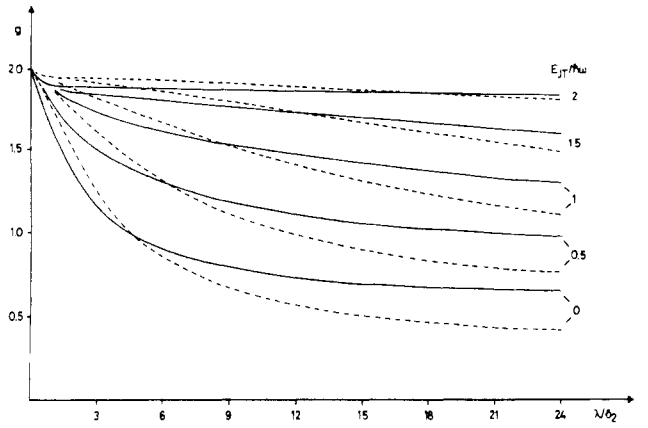

Figure 7. g vs. λ/δ_2 curves for different $E_{JT}/\hbar\omega$ ratios—nonadiabatic ligand field model with $(T + E) \otimes \epsilon$ vibronic coupling ($\lambda = k_c \cdot \lambda_0$ ($k_c = 0.6$); $\Delta = 11\,900$ cm^{-1}; dashed and full curves corresponding to $g_\parallel$ and $g_\perp$, respectively; $E_{JT} \simeq 1.5\hbar\omega$ and $\lambda \simeq 23\delta_2$ refer to Cs_2KTiCl_6).

ponents on the basis of pure group theoretical methods will be published separately by one of us.[14] The energies of the three lowest vibronic states are depicted in Figure 6 as a function of the linear Jahn–Teller coupling E_{JT} (in $\hbar\omega$) for different values of the static ligand field parameter δ_2. The limits $E_{JT} \to 0$ and ∞ would correspond to the ligand field model of Figure 5—with vibronically quenched LS coupling in the latter case, however. Figure 7 shows g values, calculated with this model, in dependence on λ/δ_2 ($\lambda = k_c\lambda_0$; $k_c = 0.6$) for different $E_{JT}/\hbar\omega$ ratios. We obtain the following energies for Cs_2KTiCl_6

$$3\delta_2 \simeq 15 \text{ cm}^{-1} \qquad E_{JT} = 1.5\ \hbar\omega \tag{4}$$

which differ greatly from those obtained from the adiabatic calculation. The observed distinct band splitting, $\Delta E = 1400$ cm^{-1}, of the excited ^2E_g state can hardly be caused by the tiny static compression of the $TiCl_6^{3-}$ polyhedra but is obviously induced by the vibronic interaction of the ϵ mode with this electronic state (dynamic Jahn–Teller $E \otimes \epsilon$ coupling). The corresponding coupling energy E_{JT}' can be estimated from[15]

$$\Delta E(^2E_g) = 2(E_{JT}'\hbar\omega \cot h\ (\hbar\omega/kT))^{1/2} \tag{5}$$

One obtains an energy $E_{JT}' \simeq 7\ \hbar\omega$, which is larger than the one in the ground state by a factor of about 5. This is expected, because the T_{2g} state is only π antibonding and hence less strongly coupled to the ligand environment than the σ-antibonding E_g state. In the case of octahedral Cu^{2+} with static Jahn–Teller distortions and a reversed energy level sequence the E_{JT}'/E_{JT} ratio is of about the same magnitude ($\simeq 4 \pm 1$).[3]

There are only two other cases reported for octahedral Ti^{3+} where a dynamic Jahn–Teller effect is unambiguously established. Ti^{3+}, doped into the cubic methylammonium alum $CH_3NH_3Al(SO_4)_2 \cdot 6H_2O$, occupies a slightly trigonally compressed octahedral host site. This static crystal field leads to the same $_a\Gamma_7$ ground state as in our case and induces the **g** tensor $g_\parallel = 1.37$ (1) and $g_\perp = 1.61$ (1).[16] The average g value of 1.53 is similar to ours, and we may also deduce a $E_{JT}/\hbar\omega$ ratio of around 1.5 from Figure 7—though the $Ti(OH_2)_6^{3+}$ polyhedron gives rise to somewhat different ligand field parameters from those of $TiCl_6^{3-}$. In agreement with this number the calculated ratios[16] are 1.73 and 1.39, depending on the experimental data used. Ti^{3+} doped into the corundum lattice of α-Al_2O_3 is again the subject of a static, host-lattice-induced distortion, which is trigonal. It is more distinct in this case, however, and has the sign of an elongation. The $_b\Gamma_7$ doublet (Figure 5) is now lowest and should induce quite different g parameters (first order only): $g_\parallel = g_0 - 2k$ and $g_\perp = 0$.[8] The experimental values ($g_\parallel = 1.07$, $g_\perp < 0.2$) again indicate a reduction due to a only): $g_\parallel$ ϵ vibronic coupling. The calculated $E_{JT}/\hbar\omega$ ratio of 1.56[17] is of the same magnitude as for the Cl^- and H_2O ligands.

c. The structural, spectroscopic, and magnetic measurements on the model systems $A_2A'TiCl_6$ give evidence that the $TiCl_6^{3-}$ octahedra show vibronic $T \otimes \epsilon$ coupling effects of remarkable strength ($3E_{JT} \simeq 1100$ cm^{-1} for $\hbar\omega = 250$ cm^{-1}). This coupling is also evident in the excited ^2E_g state ($3E_{JT}' \simeq 5000$ cm^{-1}). The observed tiny static distortion component is induced by geometric packing forces. The dynamic Jahn–Teller coupling is comparable in strength to the one in Ti^{3+}-doped alum and α-Al_2O_3.[16,17] Though we have investigated a pure Ti^{3+} compound, a cooperative effect is apparently not present. Neither an increase of the $E_{JT}/\hbar\omega$ ratio nor a transition to a phase with statically Jahn–Teller distorted octahedra has been found when the temperature is lowered. We may conclude that σ-antibonding E_g ground states in octahedral coordination undergo much more significant Jahn–Teller interactions than the π-antibonding T_{2g} states in the same coordination geometry. Though quite strong dynamic coupling effects are present in the latter case, E_{JT} is larger by a factor of at least 5 for d^9, d^4, and low-spin d^7 cations (Cu^{2+}, Ag^{2+}, Cr^{2+}, Mn^{3+}, and low-spin Co^{2+} and Ni^{3+})[3,4] and static deformations are usually observed, which are indeed expected for $E_{JT} >> \hbar\omega$.

Acknowledgment. We owe thanks to Dr. H. Homborg (University of Kiel) for the Raman spectra of Cs_2KTiCl_6 and $Rb_2NaTiCl_6$ as well as for fruitful discussions.

Registry No. I, 97135-60-9; II, 97135-61-0; III, 16449-04-0.

(14) S. Kremer, to be submitted for publication.
(15) Y. Perlin and E. Perlin, *Sov. Phys.—Solid State(Engl. Transl)*, **10**, 1531 (1969); M. Wagner, *Phys. Lett. A*, **29A**, 472 (1969).
(16) N. Rumin, C. Vincent, and D. Walsh, *Phys. Rev.B: Solid State*, **7**, 1811 (1973); Y. H. Shing, C. Vincent, and D. Walsh, *Phys. Rev. B: Solid State*, **9**, 340 (1974).
(17) R. M. Macfarlane, J. Y. Wong, and M. D. Sturge, *Phys. Rev.*, **166**, 250 (1966).